

N O T I C E

THIS DOCUMENT HAS BEEN REPRODUCED FROM
MICROFICHE. ALTHOUGH IT IS RECOGNIZED THAT
CERTAIN PORTIONS ARE ILLEGIBLE, IT IS BEING RELEASED
IN THE INTEREST OF MAKING AVAILABLE AS MUCH
INFORMATION AS POSSIBLE

9950 - 539

(NASA-CR-164343) NASA-CASI/JPL HIGH
EFFICIENCY THERMICNIC CONVERSION STUDIES
Executive Summary Report (Thermo Electron
Corp.) 57 p HC A04/MF A01 CSCL 10A

N81-24528

Unclas

G3/44 42376



 **Thermo
Electron**
CORPORATION

TE4247-193-81

TECHNICAL SUMMARY REPORT
NASA-OAST /JPL
HIGH EFFICIENCY THERMIONIC
CONVERSION STUDIES

JPL Contract No. 955009

March 1981

Prepared by
Thermo Electron Corporation
101 First Avenue
Waltham, Massachusetts 02254

TABLE OF CONTENTS

I.	INTRODUCTION AND SUMMARY	1
II.	THERMIONIC CONVERTER CHARACTERIZATION	5
III.	OXYGEN TRANSPORT FROM AN OXIDE COLLECTOR	27
IV.	CYLINDRICAL CONVERTER COMPONENT DEVELOPMENT ...	35
V.	SYSTEM CONSIDERATIONS	47

PRECEDING PAGE BLANK NOT FILMED

I. INTRODUCTION AND SUMMARY

This report summarizes the technical effort on the NASA-OAST/JPL thermionic converter studies at Thermo Electron during 1980. The primary goal of this program was to develop thermionic energy conversion (TEC) technology appropriate for nuclear electric propulsion (NEP) missions. This space TEC effort was complementary to the terrestrial TEC studies sponsored by the Department of Energy (DOE), which have the goal of topping fossil fuel powerplants. Since the technical details of the combined space and terrestrial investigations are available in the joint DOE/JPL Advanced Thermionic Technology Program Progress Report Nos. 42, 43, 44, and 45 - this document (consistent with instructions from Dr. Katsunori Shimada of JPL) will be essentially an executive summary report.

TEC has been a primary conversion option for space reactors because of its: (1) high operating temperature, (2) lack of moving parts, (3) modularity, (4) established technology and 5) development potential.

During 1980, the primary focus of the NASA/OAST/JPL program was on characterization of promising emitter-collector pairs. The Progress Reports cited previously contain a great deal of data on thermionic diode outputs at the reference emitter temperature of 1650 K as a function of collector temperature, cesium reservoir temperature, and interelectrode spacing for a variety of electrode combinations. These data are summarized in Section II of this report.

The salient result is that thermionic converters (constructed with collectors formed by molybdenum sublimation in an oxygen atmosphere onto a niobium substrate) can be reproducibly built with performances corresponding to a mean barrier index of 2.0 eV. At an emitter temperature of 1650 K and the collector temperature ranging between 750 and 900 K, this measured performance corresponds to a power density of over 5 W/cm² at a calculated electrode efficiency of around 12 percent. An interesting result is that for converters built with sublimed molybdenum oxide collectors, molybdenum and tungsten emitters gave comparable outputs. Based on these results, state-of-the-art TEC performance corresponds to a barrier index of 2.0 eV. This represents an improvement of about 0.1 eV during the past two years.

Significant progress was made in understanding that the oxygen transport mechanism was associated with sublimed molybdenum oxide collectors. Based on mass spectroscopy measurements, Auger spectroscopy, thermochemical analyses, and converter data summarized in Section III, it appears that the oxygen transport from the collector to the emitter is via Cs_2O formed by cesium diffusion and reaction with the molybdenum oxide in the sublimed coating. This insight may lead to improved converter operation.

Development of cylindrical converter components received a secondary effort. In spite of the low program emphasis, two results are noteworthy. First, a leaktight prototype niobium bellows was fabricated. Second, a technique was developed for casting sapphire between molybdenum cylinders with diameters prototypic of the molybdenum-lithium heat pipes and molybdenum emitters projected in the JPL-LASL TEC reactor design. The temperature drop across the sapphire was only 14 K at a heat flux of about 30 W/cm^2 . Although the stability of the electrical resistivity was marginal, the results are encouraging that the heat pipe insulation problem can be solved. In particular, the stable operation of silicon carbide-carbon-tungsten structures at a temperature of 1730 K for over

5900 hours in the DOE TEC program suggest that silicon carbide is a promising candidate for this application. The component development effort is discussed in Section IV.

System studies summarized in Section V indicate that if the heat pipe-emitter insulation problem can be resolved at 1650 K, specific mass values of approximately 20 kg/kWe can be expected with a TEC out-of-core reactor system. If this insulation problem cannot be resolved, results presented in this section suggest that radiation coupling of the heat pipe to the thermionic converters constitutes a viable system option that deserves further exploration.

In summary, the substantial technical progress in this program demonstrates TEC as a viable conversion system for reactor space power applications provided that a suitable emitter temperature (≥ 1650 K) can be supplied.

II. THERMIONIC CONVERTER CHARACTERIZATION

Candidate emitter and collector pairs were characterized for the operational temperatures of primary interest for nuclear electric propulsion (NEP). Converter performances were measured at the reference emitter temperature, T_E , of 1650 K as a function of collector temperature, T_C , cesium temperature, T_R , and interelectrode spacing, d .

A. Research Converter Description

The basic configuration of all the thermionic converters used in these studies is shown in Figure 1. Details of design and fabrication depend on the electrode materials in a particular diode. In a few cases, sapphire windows were incorporated into the converters in order to observe the electrodes and discharges. The nickel bellows permits the emitter-collector spacing to be varied from 0.1 to 2 mm. The converter is mounted in a test stand, which allows the J-V characteristics to be measured as a function of T_E , T_C , T_R , and d without removing the bell jar enclosing the test stand.

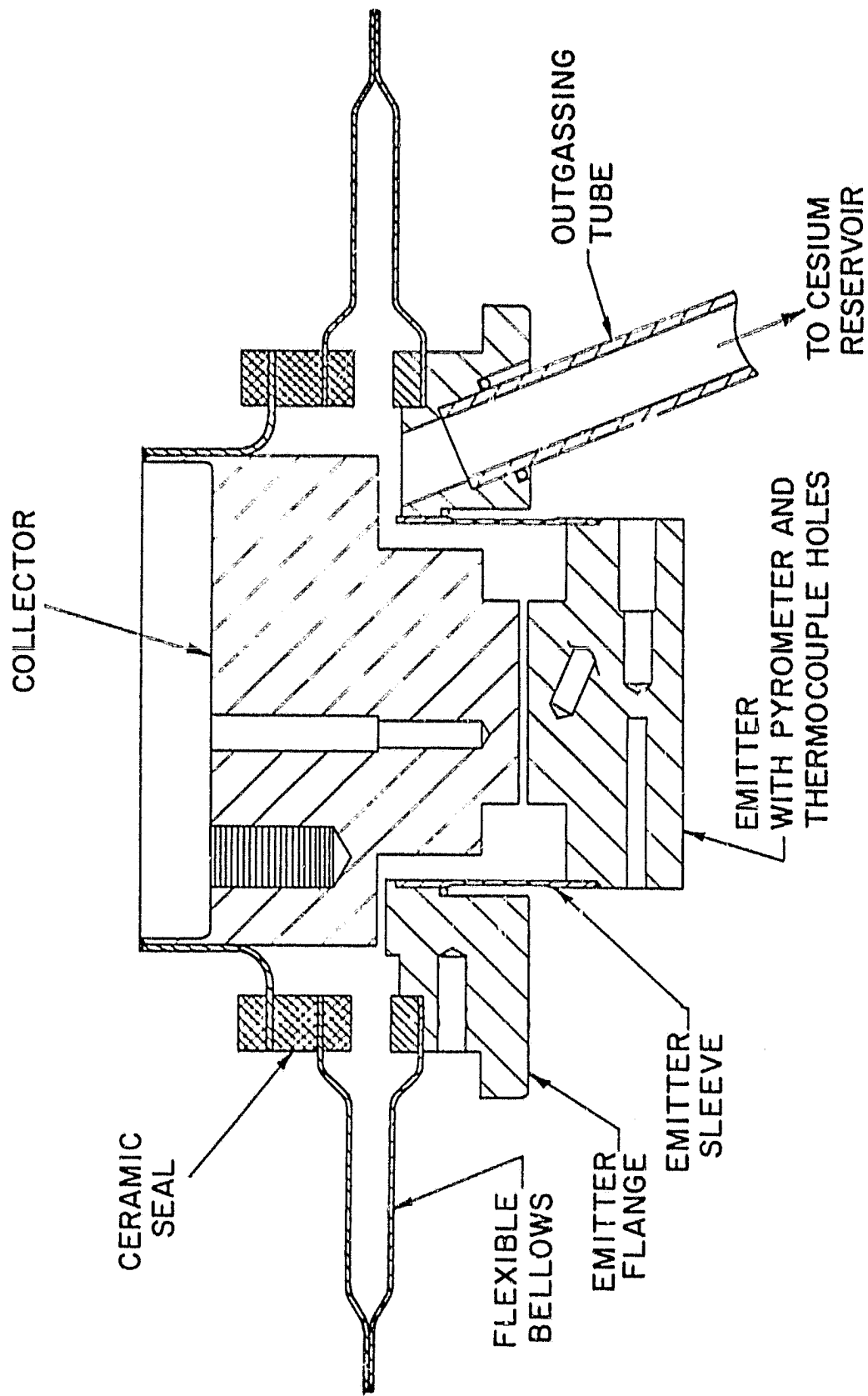


Figure 1. Planar, Variable Spacing Research Converter

The reference out-of-core thermionic reactor system has an emitter temperature, T_E , of 1650 K. System constraints such as the output electrical power, dimensions of the space shuttle bay, maximum allowable specific power (i.e., kg/kWe), interface temperature drops, and radiator heat pipe characteristics will be used in combination with data on thermionic converter output as a function of collector temperature, T_C , to determine the collector temperature most appropriate for the system. Recent studies indicate that the optimum T_C will probably range between 800 and 1000 K. However, the power density, P_D , and efficiency characteristics of the thermionic converter are sensitive to collector temperature in this range and must be better defined in order to establish the design value of T_C . This problem is complex since, for a given emitter and collector pair, P_D is a function of T_E , T_C , the current density, J , the interelectrode spacing, d , and the cesium pressure, P_{CS} , (which corresponds to the liquid cesium reservoir temperature, T_R). Sometimes an additional constraint is placed on the output voltage, V , or the current density. The measurements during this program period provide a data base that can be correlated

with models of the thermionic converter used in the system studies. Since the T_E value of 1650 K appeared to be well established for the NEP mission, most of the converter data were taken at this temperature.

B. Test Converter Summary

A summary of the JPL converters in this test series is given in Table I. The most significant result is the good performance obtained with most of the converters built with sublimed molybdenum oxide collectors. The average minimum barrier index, V_B , of JPL Converter Nos. 4, 9, 10, 11, 14, and 15 with molybdenum oxide collectors was 2.01 eV.

C. Performance Characteristics

The performance of Converter No. 232 (JPL No. 4) was typical of the converters with well activated molybdenum oxide collectors. Thus, the data from this thermionic diode will be presented as a representative of such converters. Converter No. 232 had an electropolished (EP) arc cast molybdenum emitter and a sublimed molybdenum oxide collector. It was built with a sapphire window which allowed observation of the electrode region. The window was cooled by a copper sleeve that was coupled to a heat sink via copper cooling straps.

TABLE I
SUMMARY OF JPL CONVERTER TESTS

JPL NO.	TECO NO.	EMITTER MATERIAL	COLLECTOR MATERIAL (ppm Oxygen)	Min V_B eV	Min T_C eV	COMMENTS
1	227	Mo	Nb	2.30	-	V_B measured as a function of T_C at $T_C = 800$ K, $V_B = 2.30$ eV at $T_C = 1100$ K, $V_B = 2.40$ eV Reported in 1979.
2	223	Mo	W_xO_y	2.10	1.60	Window Diode Converter established that an oxide collector helps a Mo emitter. Reported in 1979.
3	231	Mo	Mo_xO_y (1,100)	2.28	1.94	Window Diode V_B measured as a function of T_C at $T_C = 800$ K, $V_B = 2.28$ eV at $T_C = 1100$ K, $V_B = 2.45$ eV
4	232	EP Mo	Mo_xO_y (11,000)	1.98	1.50	Window Diode V_B measured as a function of T_C at $T_C = 750$ K, $V_B = 1.98$ eV at $T_C = 900$ K, $V_B = 2.12$ eV
5	233	Mo/Rc	Ni	2.17	-	Window Diode/ 1/2" pumpout Hybrid emitter - fine structure. Hybrid mode not observed - shipped to JPL.
6	219	LaB_6	LaB_6			Very little output power.
7	234	EE-FW	Nb	2.12	1.55	V_B measured as a function of T_C at $T_C = 800$ K, $V_B = 2.12$ eV at $T_C = 1000$ K, $V_B = 2.40$ eV

TABLE I (Continued)

JPL NO.	TECO NO.	EMITTER MATERIAL	COLLECTOR MATERIAL (ppm Oxygen)	Min V_B eV	Min ϕ_C eV	COMMENTS
9	236	EE-FW	Mo _x O _y (1,800)	2.06	1.67	V_B measured as a function of T_C at $T_C = 800$ K, $V_B = 2.06$ eV at $T_C = 1000$ K, $V_B = 2.30$ eV Installed in life test station.
10	240	EE-FW	Mo _x O _y (1,800)	1.98	1.54	V_B measured as a function of T_C at $T_C = 800$ K, $V_B = 1.98$ eV at $T_C = 1000$ K, $V_B > 2.40$ eV
11	241	AD-FW	Mo _x O _y (18,000)	1.98	-	Collector coating flaked
12	243	AD-Re	Mo _x O _y (18,000)	-	-	Rhenium apparently not affected by oxygen. Collector coating flaked.
13	257	EP-Mo	Mo _x O _y (12,300)	>2.2	-	No oxygen effect observed.
14	254	EE-FW	Mo _x O _y (9,880)	2.00	1.48	Stable at good performance for 200 hours.
15	249	EE-FW	Mo _x O _y (9,880)	2.06	1.58	Stable at good performance for 110 hours.
16	256	EE-FW	Mo _x O _y (12,300)	>2.2	-	No Oxygen effect observed.

Initial performance measurements of Converter No. 232 gave a high barrier index. At an emitter temperature of 1650 K, the barrier index was 2.32 eV at 5 A/cm². No pronounced increase in emitter saturation current with increasing collector temperature was evident and the initial J-V characteristics of the diode appeared to be somewhat resistive.

After approximately 30 hours of operation, the diode output improved dramatically and the barrier index decreased to 1.98 eV for $T_E = 1650$ K. The J-V characteristics at $T_E = 1650$ K, $T_C = 750$ K, and $d = 0.50$ mm are given in Figure 2 for a range of cesium reservoir temperatures from 507 to 551 K - corresponding to a cesium pressure, P_{CS} , range of 0.25 to 1.0 torr, respectively. Evidently, cesium combines with oxygen in the molybdenum matrix to form a volatile oxide a low work function (relative to a cesiated metal). Oxygen transport to the emitter provides a high current density for a given cesium pressure, which allows the interelectrode spacing to be increased. Consequently, addition of oxygen to the converter from the sublimed molybdenum oxide surface results in a higher performance with an electrode spacing that is more practical.

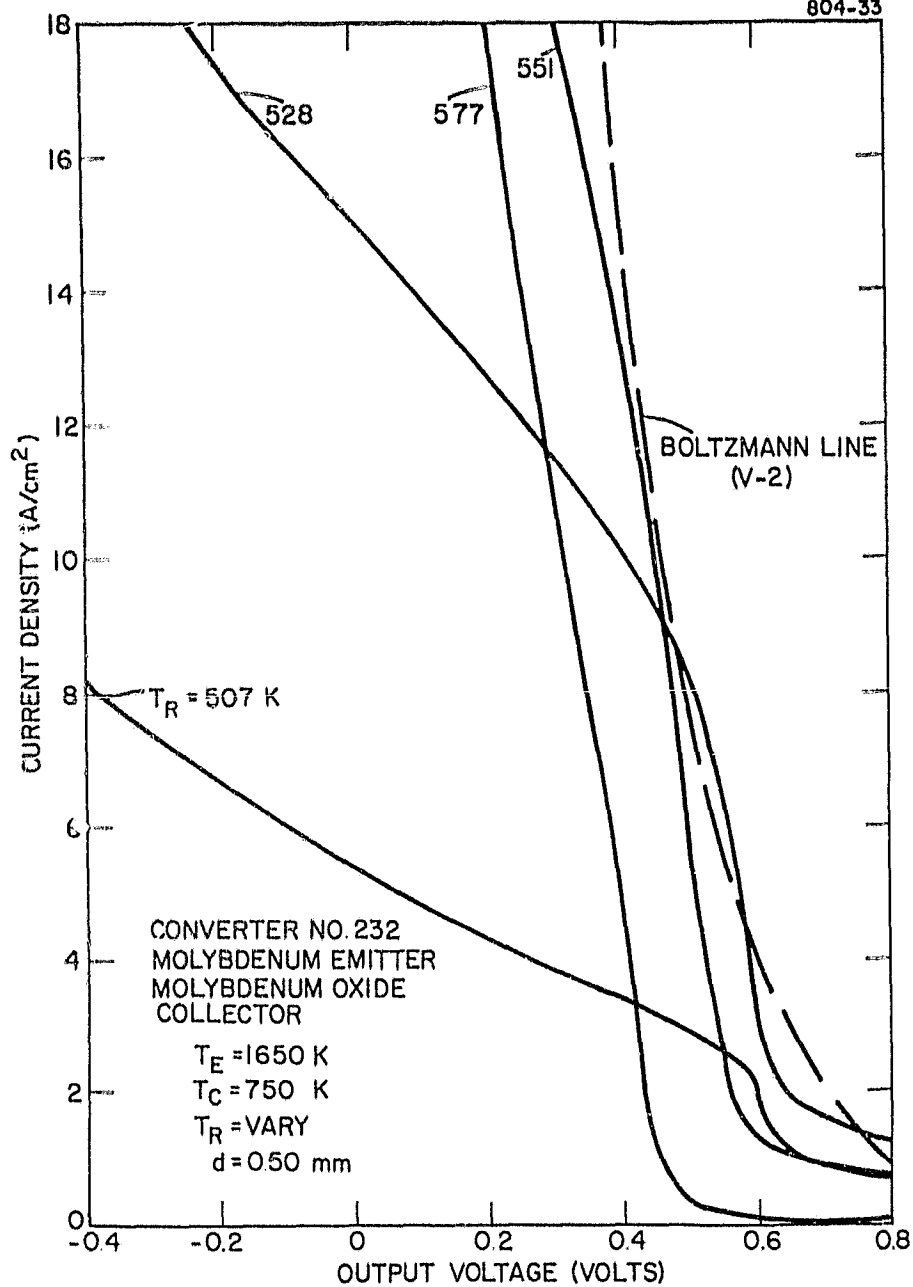


Figure 2. J-V Characteristics of Converter No, 232 as a Function of Cesium Reservoir Temperature for $T_E = 1650 \text{ K}$, and $d = 0.50 \text{ mm}$

It should be noted that the output voltage given in all the figures in this report are electrode, rather than lead, potential because the emitter sleeve (see Figure 1) is much thicker than optimum. Performance characteristics at $T_E = 1650$ K for optimized collector temperature and cesium pressure at spacings between 0.25 to 1.0 mm are given in Figure 3. As the distance between the emitter and collector increases from 0.5 to 1.0 mm, there are pronounced changes in the J-V characteristics. Measurements were also made as a function of collector temperatures. For $T_E = 1650$ K, the diode was optimized for cesium pressure and spacing at collector temperatures of 750, 800, 850, and 900 K. These results are shown in Figure 4. It is evident that the output decreases significantly as the collector temperature goes above 850 K.

A More typical performance was observed for Converter No. 226 (see Figure 5). A barrier index of 2.1 eV, or less, was maintained at collector temperatures up to 1000 K. This converter had an EP CVD fluoride tungsten emitter which was highly oriented (100). The collector was polycrystalline nickel.

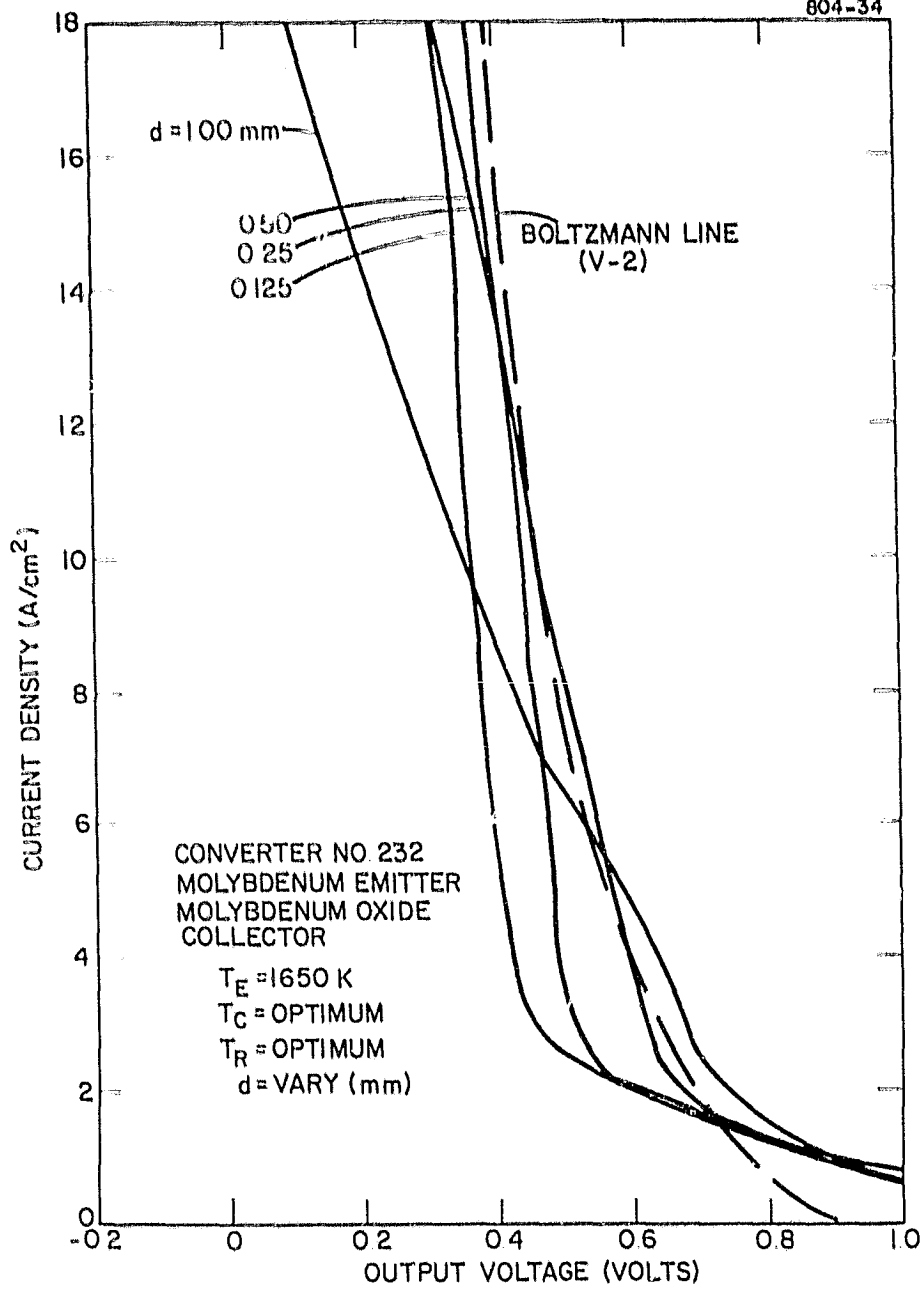


Figure 3. Cesium and Collector Temperature Optimized Performance of Converter No. 232, Parametric in Spacing, for $T_E = 1650$ K.

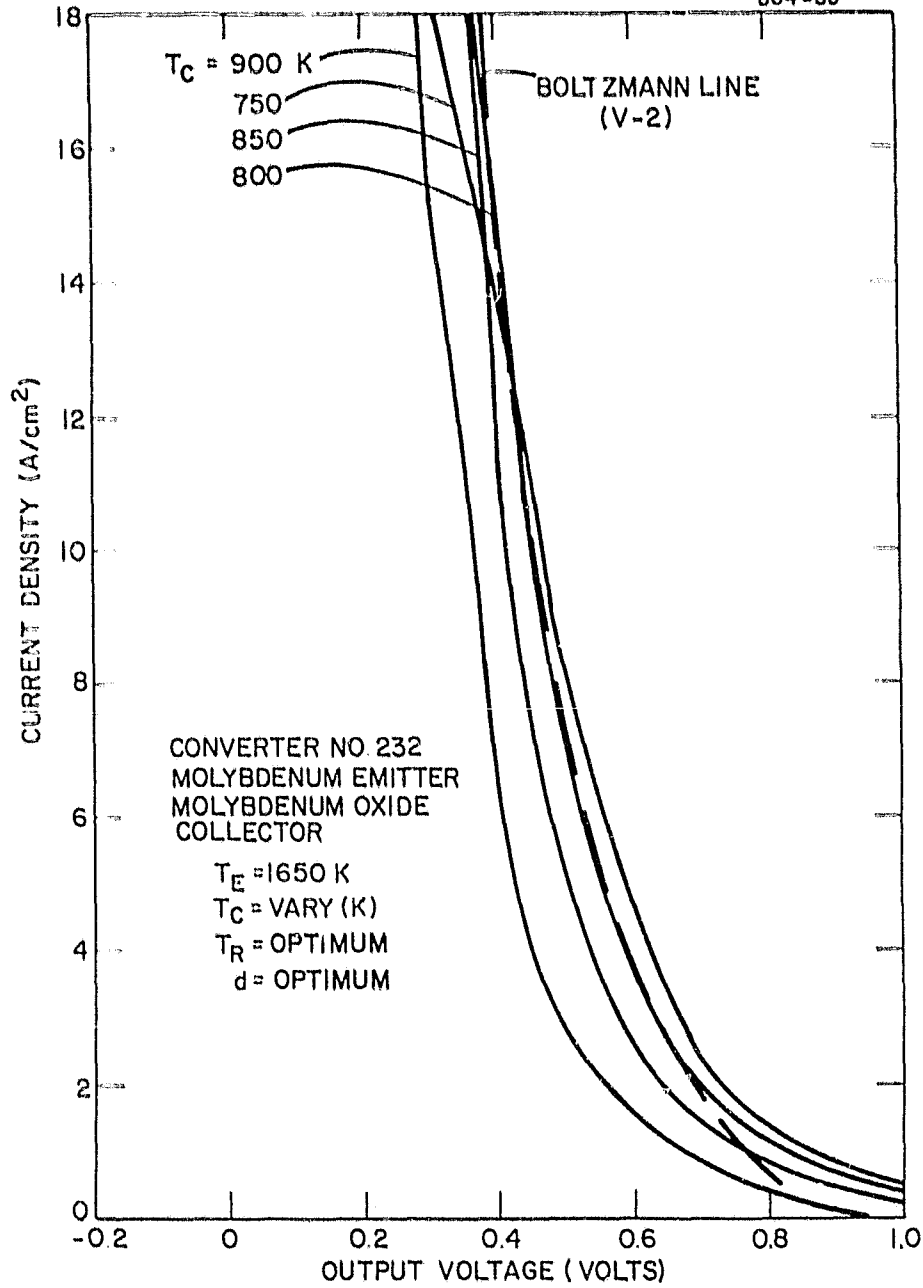


Figure 4. J-V Characteristics of Converter No. 232 for Optimized Cesium Pressure and Interelectrode Spacing, Parametric in Collector Temperature, for $T_E = 1650$ K.

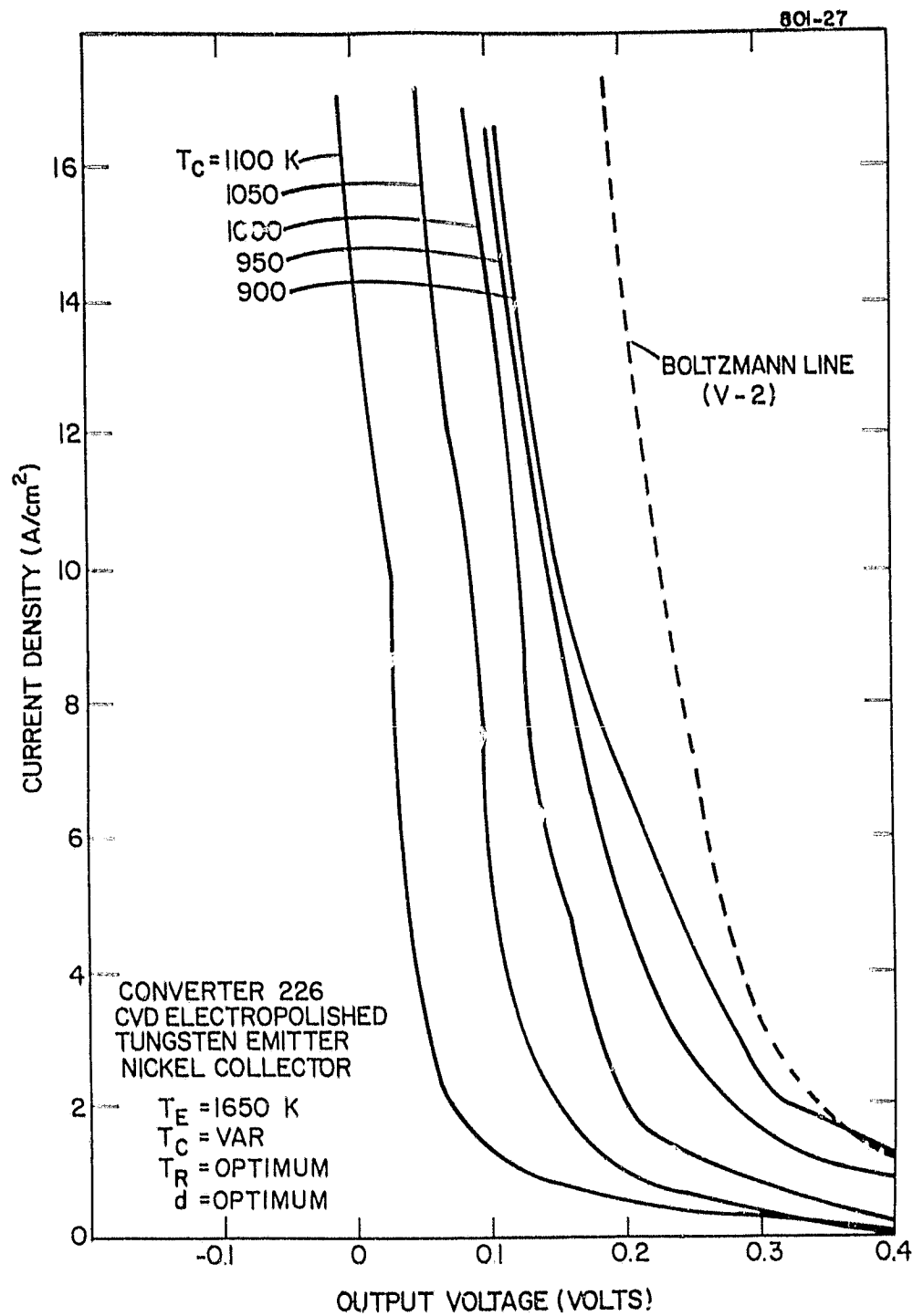


Figure 5. J-V Characteristics of Converter No. 226, Parametric in Collector Temperature, for $T_E = 1650 \text{ K}$ and Optimized T_R and d .

It is interesting to compare the output of Converter No. 226 with that of its sister diode, Converter No. 225, which also had a nickel collector. However, the emitter of Converter No. 225 was as deposited (AD) CVD fluoride tungsten. The J-V characteristics for Converter No. 225 are shown in Figure 6. Over the collector temperature range from 900 to 1000 K, the performance of Converter No. 226 was much higher than that of Converter No. 225.

The diode that was least sensitive to collector temperature was Converter No. 227 which had a molybdenum emitter and a niobium collector. The optimized J-V characteristics for this diode are given in Figure 7. Although its output is lower at $T_C = 900$ K than any other converter in this study, its output at $T_C = 1100$ K is higher.

D. Discussion

The foregoing plots of J-V characteristics versus collector temperature should be useful for out-of-core thermionic reactor design efforts. However, these raw data are not convenient for comparing the performances of the converters being evaluated. A more transparent display of the experimental results is shown in Figure 8.

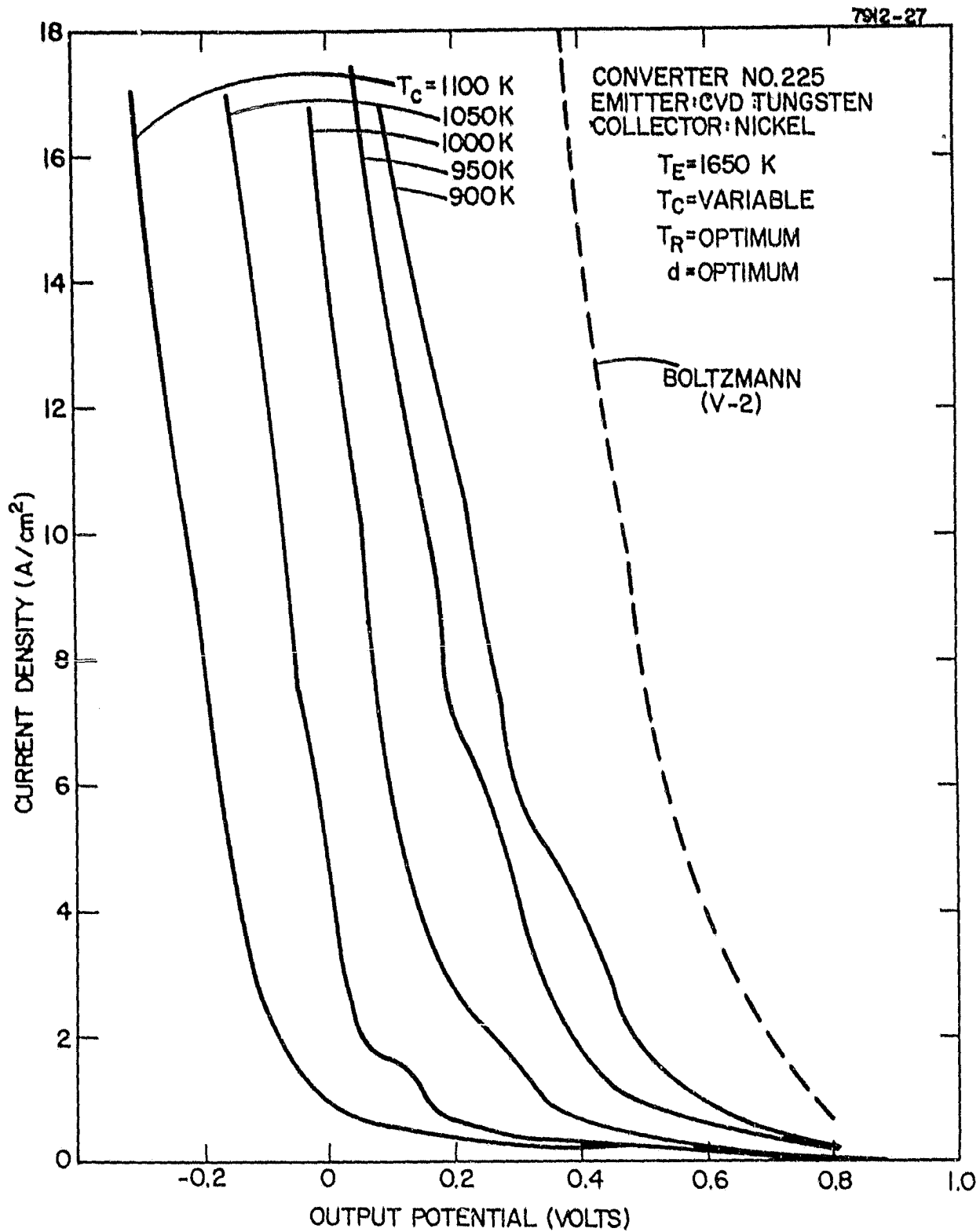


Figure 6. J-V Characteristics of Converter No. 225, Parametric in Collector Temperature, for $T_E = 1650 \text{ K}$ and Optimized T_R and d .

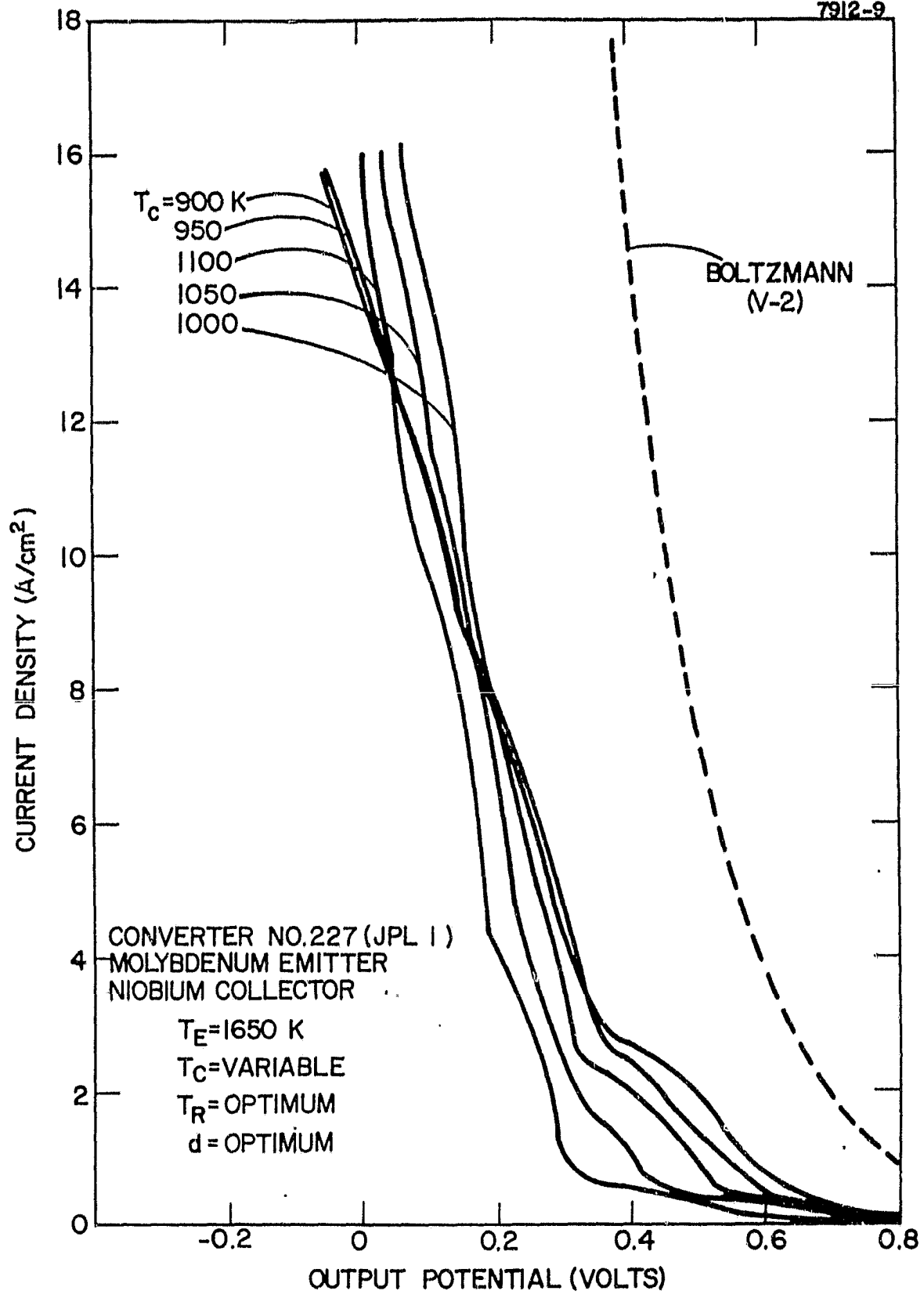


Figure 7. J-V Characteristics of Converter No. 227, Parametric in Collector Temperature for $T_E = 1650$ K and Optimized T_R and d .

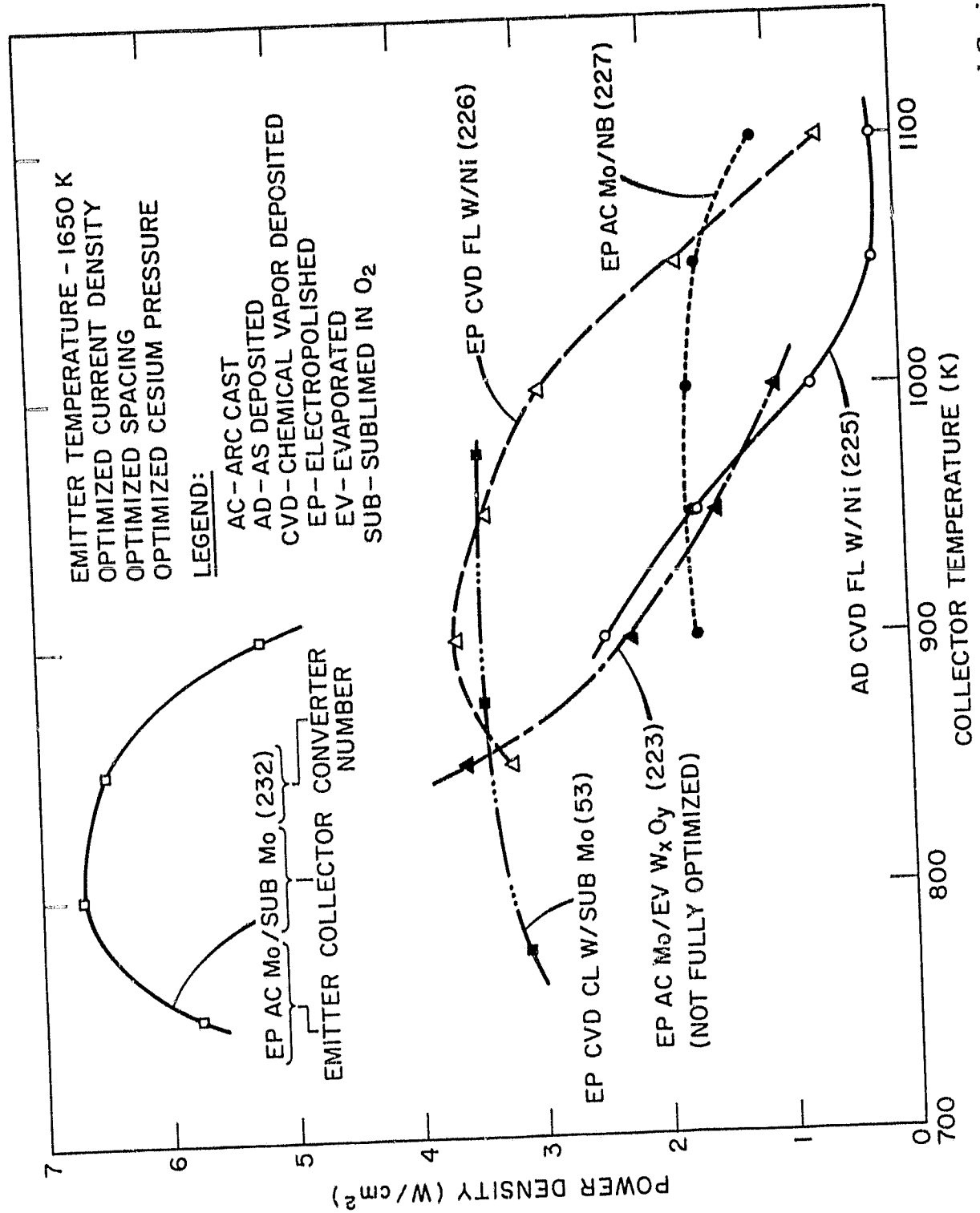


Figure 8. Power Density as a Function of Collector Temperature for Optimized Spacing and Cesium Pressure at $T_E = 1650$ K for a Variety of Research Converters (see Table I).

This figure gives the maximum output power density (for optimized current density, spacing, and cesium pressure) as a function of collector temperature for all the converters evaluated in this study. For $T \leq 900$ K, the performance of Converter No. 232 is clearly superior to that of the other diodes. Surprisingly, the output of Converter No 226, with an EP CVD fluoride tungsten emitter, is relatively high for collector temperatures up to 1050 K. As noted previously, Converter No. 227 (with an EP arc cast molybdenum emitter and a niobium collector) had the lowest power density at $T_C = 900$ K, but the highest at $T_C = 1100$ K.

Of course, the data in Figure 8 for optimized current density and optimized interelectrode spacing may correspond to impractical values of these parameters for space system applications. Therefore, a comparison is made in Figure 9 subject to the constraints of $d \geq 0.25$ mm and $J = 8$ A/cm². Although the order of converter performance is the same in both Figures 3 and 9, the power densities of most of the diodes are tested and reduced significantly by these constraints. In particular, the relatively outstanding performance of Converter No. 232 in Figure 8 is much less dramatic in Figure 9.

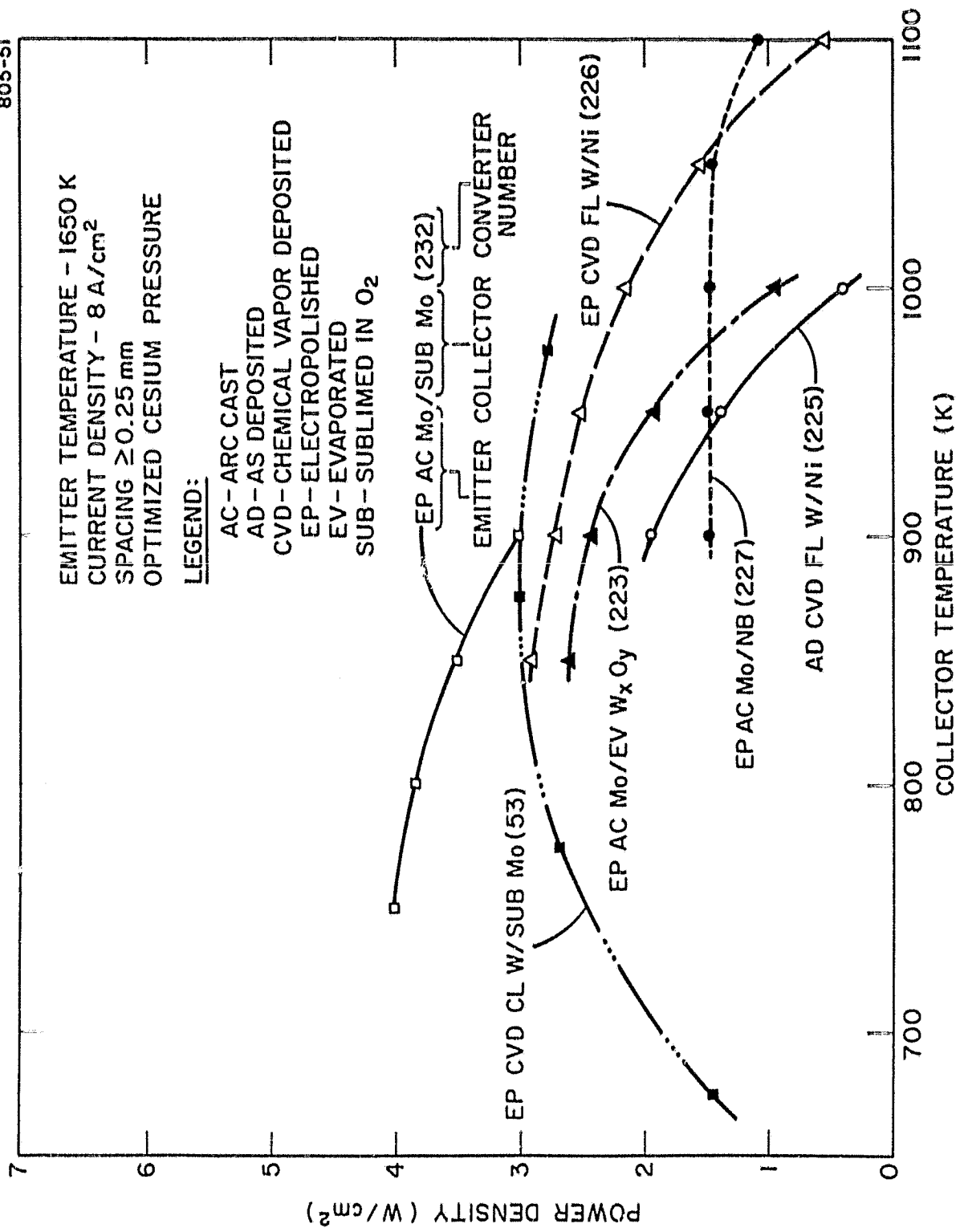


Figure 9. Power Density as a Function of Collector Temperature for Optimized Cesium Pressure and Spacings Greater Than 0.25 mm at $T_E = 1650$ K for a Variety of Research Converters (see Table I).

The converter data presented herein do not appear to be amenable to interpretation by an elementary analytical mode of the ignited mode diode. However, it is significant that the two best performing diodes (i.e., Converter Nos. 232 and 53) for $T_C \leq 900$ K both utilized sublimed molybdenum oxide collectors.

It is quite interesting to compare the outputs of Converter Nos. 225 and 226, both of which had nickel collectors. At all collector temperatures, the performance of Converter No. 226 (with an EP CVD fluoride tungsten emitter) is far more superior to that of Converter No. 225 (with an AD CVD fluoride tungsten emitter) whose emitter is highly structured. Therefore, these data are not consistent with the results of Rasor Associates who have reported better performance with a structured emitter.

The quite different outputs of Converter No. 225 and 226 are surprising since, from a simple thermionic converter model, the variation in power density with collector temperature is expected to be similar for ostensibly identical nickel collectors. Although both collectors were machined from the same block of 201 nickel, fabrication and outgassing procedures may have differed in subtle, but significant, respects.

Postoperational diagnostics on the emitter of these two converters did not clarify the discrepancy in their performances. After heating to 1400 K, the elemental surface composition of the emitter from Converter No. 225 was, approximately: W(84%), O(14%), and C(2%).

For comparison, the composition of the emitter from Converter No. 226 was: W(63%), O(36%), and Si₂O (<1%). It was expected that the highly oxygenated emitter (i.e., Converter No. 225) would have the higher bare work function as measured by the field emission retarding potential (FERP) technique. As expected, the FERP work function (measured after heating to 1800 K) of the emitter from Converter No. 225 of 5.37 eV was higher than that from Converter No. 226 of 4.85 eV. Typically, the emitter with the higher bare work function would be expected to give the best results. However, this expectation was not realized in the data from Converters No. 225 and 226.

E. Conclusions

The output power density measured as a function of collector temperature (at a fixed emitter temperature of 1650 K) do not appear to be amenable to interpretation by

an elementary model of the ignited mode diode. For collector temperatures below 900 K, converters built with sublimed molybdenum oxide collectors give the best performance. However, the data do not imply the superiority of any particular emitter.

III. OXYGEN TRANSPORT FROM AN OXIDE COLLECTOR

The success of converters built with molybdenum oxide collectors has stimulated renewed interest in the oxygen transport mechanism. For molybdenum oxide collector temperatures greater than 750 K, an "oxygen effect" occurs; that is, an increase of collector temperature causes an increase in emitter saturation current. This is believed to be due to an oxygen containing gas being transported across the interelectrode gap and decomposing on the emitter. It is unlikely that oxygen is transported as a gas since it would be expected to react with cesium to form an oxide. This expectation is consistent with the negative results of experiments in which oxygen was introduced into operating converters through the collector (either through sintered lanthanum hexaboride or a center hole).

The following four pieces of evidence indicate that the most plausible oxygen carrier is Cs_2O . The first stated evidence is from new data and the other three factors are from previous data.

A. Mass Spectroscopy

A sublimed molybdenum oxide collector structure (from the same sublimation run as for the collector of Converter No. 232) was mounted in front of a quadrupole mass spectrometer in the SCC. Mass spectra taken as a function of sample temperature are shown in Figure Nos. 10 through 12. The temperature was measured with an optical pyrometer with an assumed collector emissivity of 0.4. Oxygen gas is not detected for any temperature. MoO_3 is first detected at 1450 K (at an estimated pressure of 10^{-11} torr). The occurrence of MoO_2 , MoO , and Mo may be due either to actual desorption from the collector or from cracking of MoO_3 in the mass spectrometer. The seven peaks corresponding to each molybdenum oxide are due to the seven major isotopes of molybdenum, and the magnitude of each peak corresponds well with the relative natural abundance of that isotope.

On the basis of these data, one can rule out oxygen gas evolved from the collector as an oxygen carrier responsible for the oxygen effect. One can also rule out molybdenum oxides evolved from the collector since the oxygen effect occurs at 750 K while molybdenum oxides are not detected until the collector temperature reaches 1450 K.

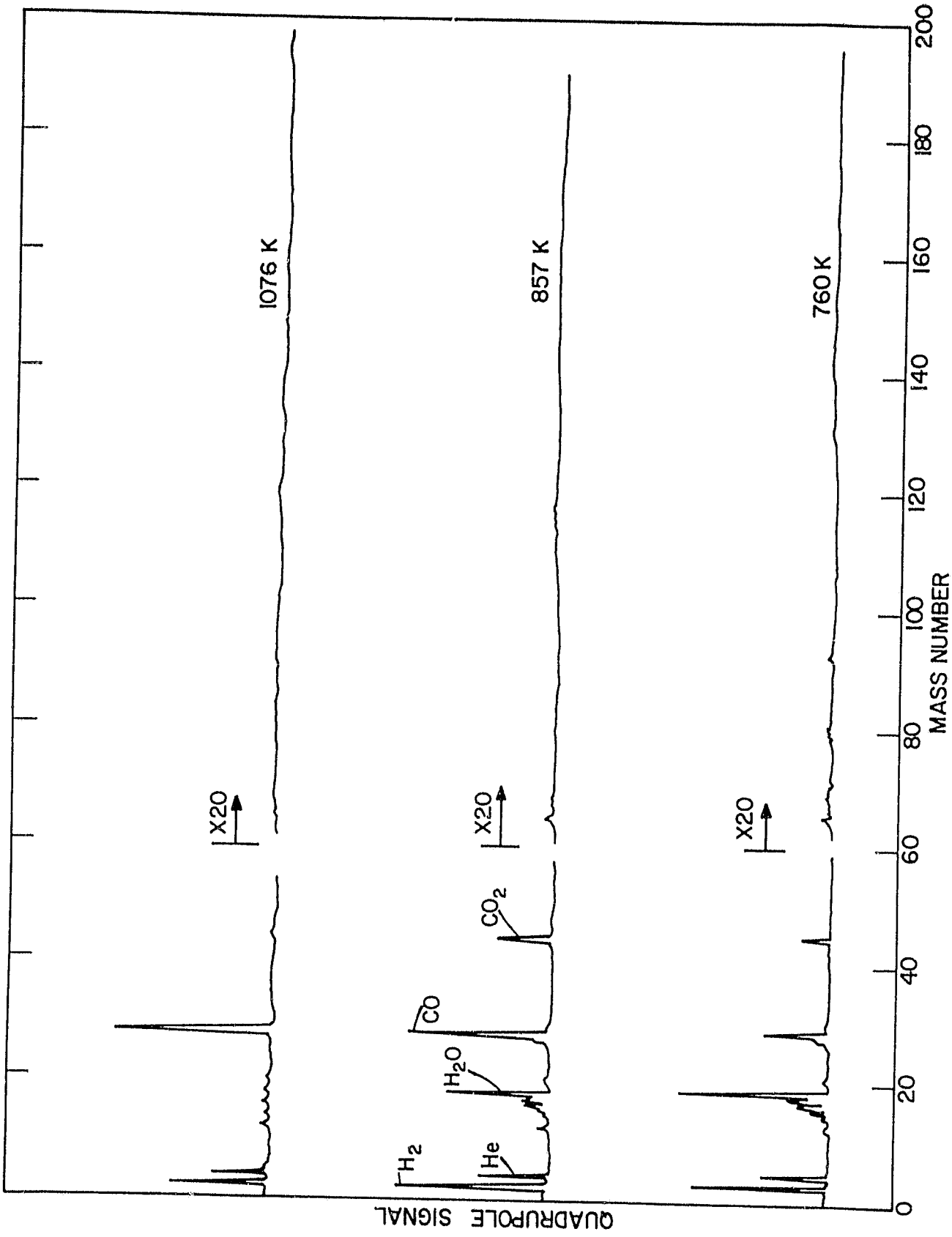


Figure 10. Quadrupole Signal vs Mass Number of a Sublimed Molybdenum Oxide Collector Heated to Temperatures of 760, 857, and 1076.

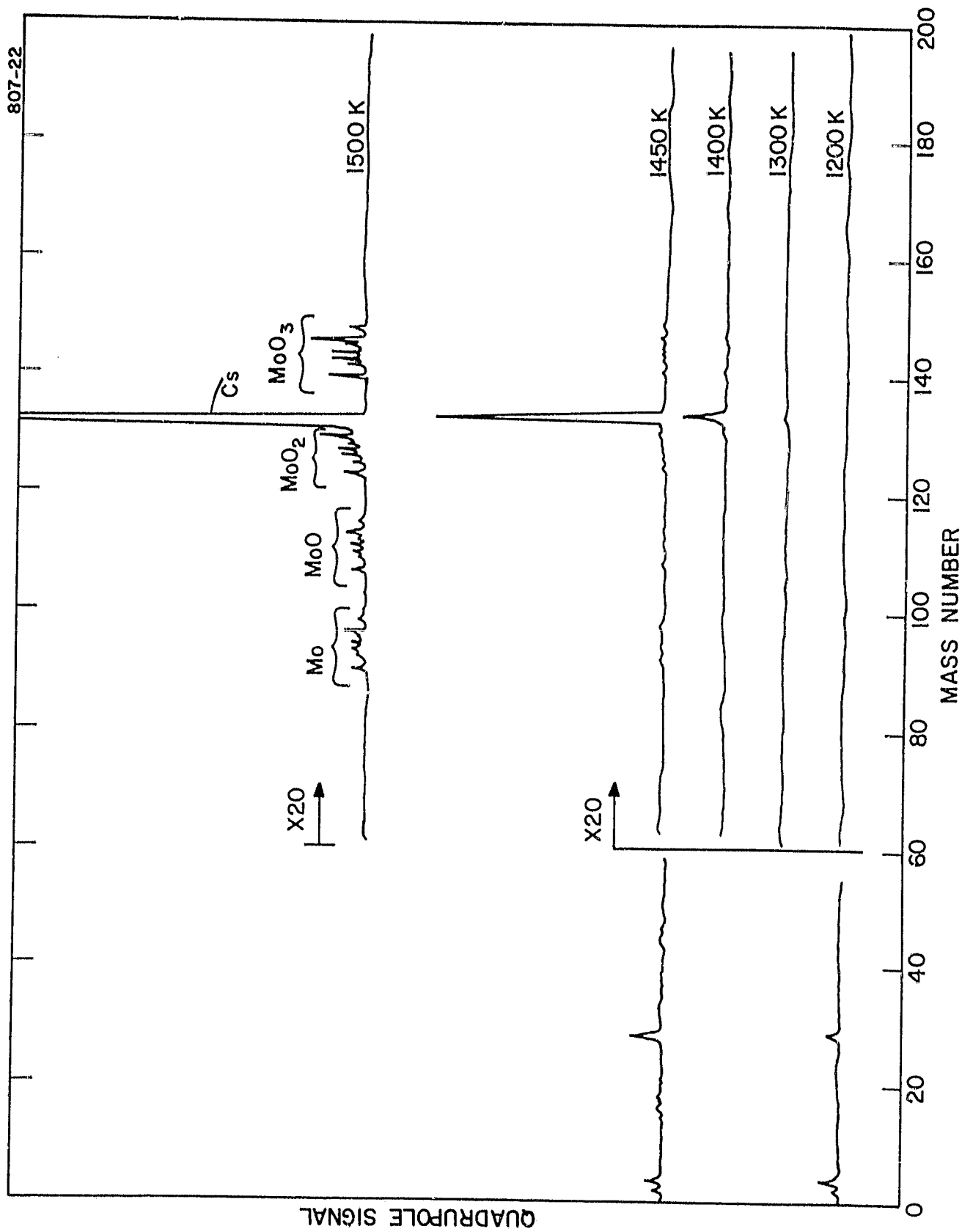


Figure 11. Quadrupole Signal vs Mass Number for a Sublimed Molybdenum Oxide Collector Heated to Temperatures of 1200, 1300, 1400, 1450, and 1500 K.

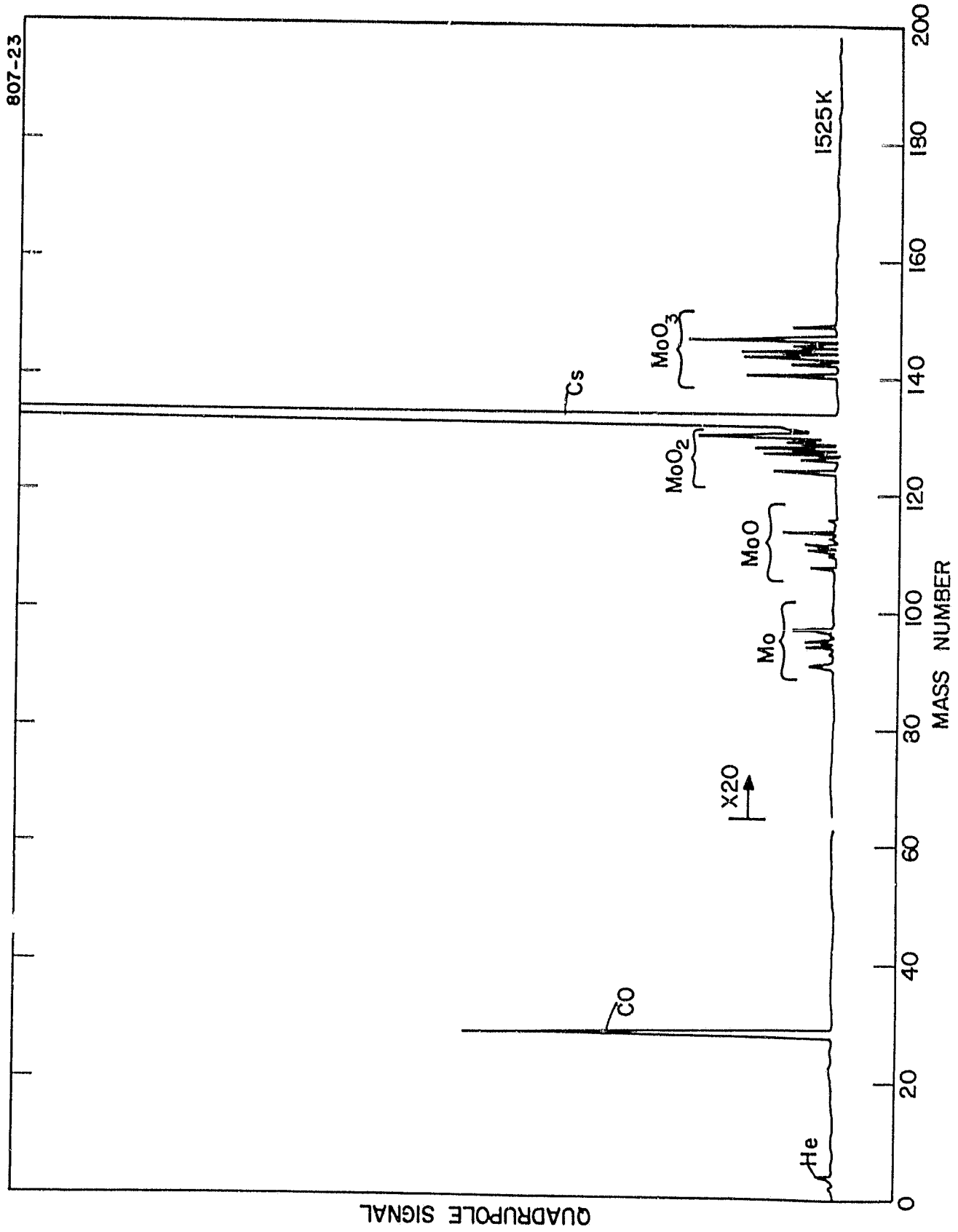


Figure 12. Quadrupole Signal vs Mass Number for a Sublimed Molybdenum Oxide Collector Heated to a Temperature of 1525 K.

B. Auger Spectroscopy

Postoperational analysis of Converter No. 210 (tungsten emitter, sublimed molybdenum oxide collector) showed no molybdenum on the emitter. The detectability limit was 1% of a monolayer. This result also supports the conclusion that molybdenum oxides evolved from the collector are not responsible for the oxygen effect.

C. Thermochemical Analysis

A thermochemical analysis for a tungsten-tungsten oxide converter reported in Progress Report No. 20 is summarized and presented in tabular form in Table II. The elemental species concentrations are 1000 moles W, 1000 moles Cs and 100 moles O. The data indicate that 89-99% of the gas is cesium, with the remainder almost entirely Cs_2O . The formation of Cs_2O is enhanced by lower temperatures (800 K) and higher total pressures (2 torr). The data imply the Cs_2O pressure at the emitter side may be 2 to 10 times smaller than at the collector. Smaller Cs_2O pressures at the emitter are expected because of

TABLE II
 THERMOCHEMICAL DATA ANALYSIS
 Adapted from TECO Report No. 20, Feb. 1977

T(K)	P(torr)	Partial Pressures (Percents of Total Pressure)								
		Cs	Cs ₂ O	Cs ₂	CsO	WO ₃	O	O ₂	WO ₂	
800	0.23	92	8	4 x 10 ⁻³	*	*	*	*	*	*
	0.76	89	11	1 x 10 ⁻²	*	*	*	*	*	*
	2.3	89	11	4 x 10 ⁻²	*	*	*	*	*	*
1500	0.23	99	0.7	2 x 10 ⁻⁴	3 x 10 ⁻⁴	9 x 10 ⁻⁴	3 x 10 ⁻⁵	2 x 10 ⁻⁶	2 x 10 ⁻⁷	6 x 10 ⁻⁷
	0.76	98	2	7 x 10 ⁻⁴	3 x 10 ⁻⁴	3 x 10 ⁻⁴	1 x 10 ⁻⁵	6 x 10 ⁻⁶	6 x 10 ⁻⁷	2 x 10 ⁻⁷
	2.3	94	6	2 x 10 ⁻³	4 x 10 ⁻⁴	9 x 10 ⁻⁴	3 x 10 ⁻⁶	2 x 10 ⁻⁷	2 x 10 ⁻⁷	6 x 10 ⁻⁸

33

* Less than 10⁻¹⁰ percent of total pressure

Thermochemical data analysis for tungsten-tungsten oxide converter. The elemental species concentrations are 1000 moles tungsten, 1000 moles cesium and 100 moles oxygen.

Cs_2O decomposition on the emitter and formation of free oxygen and tungsten oxides. Some of the tungsten oxides vaporize, but the majority stay in the solid phase at 1500 K. In summary, the thermochemical calculations indicate that Cs_2O is the most predominant oxygen containing gas for the given concentrations of W, Cs, and O.

D. Experimental Observations

Converter experiments indicate that the temperature of the oxygen effect is relatively independent of a) whether the collector is tungsten oxide or molybdenum oxide, and b) whether the sublimed molybdenum oxide is deposited at a substrate temperature of 1025 or 1225 K. These data are consistent with the hypothesis that the temperature of the oxygen effect corresponds to the desorption temperature of Cs_2O and that the substrate acts merely as a source of oxygen to form Cs_2O .

The foregoing four pieces of evidence strongly support the conclusion that the oxygen carrier in oxide converters is Cs_2O , although one cannot completely rule out such gases as H_2O , CO , or CO_2 .

IV. CYLINDRICAL CONVERTER COMPONENT DEVELOPMENT

In order to provide the technological infrastructure for constructing a prototypic cylindrical thermionic converter at a later date, a bellows subassembly was built and electrode insulation tests were performed. The former activity was successful while the evaluation of cast alumina as an electrical insulator at an emitter temperature indicated that this material was, at best, marginal.

A. Bellows Subassembly

A bellows subassembly for use in the cylindrical prototypic converter was designed and fabricated. The bellows consisted of four convolutions, as shown in Figure 13. Each convolution consisted of a flat and a formed member to allow for the largest axial movement in the minimum space. Special electron beam welding fixtures were also designed and built, as shown in the photographs in Figures 14 and 15. The completed bellows was subjected to a number of mechanical extensions and remained leak-tight.

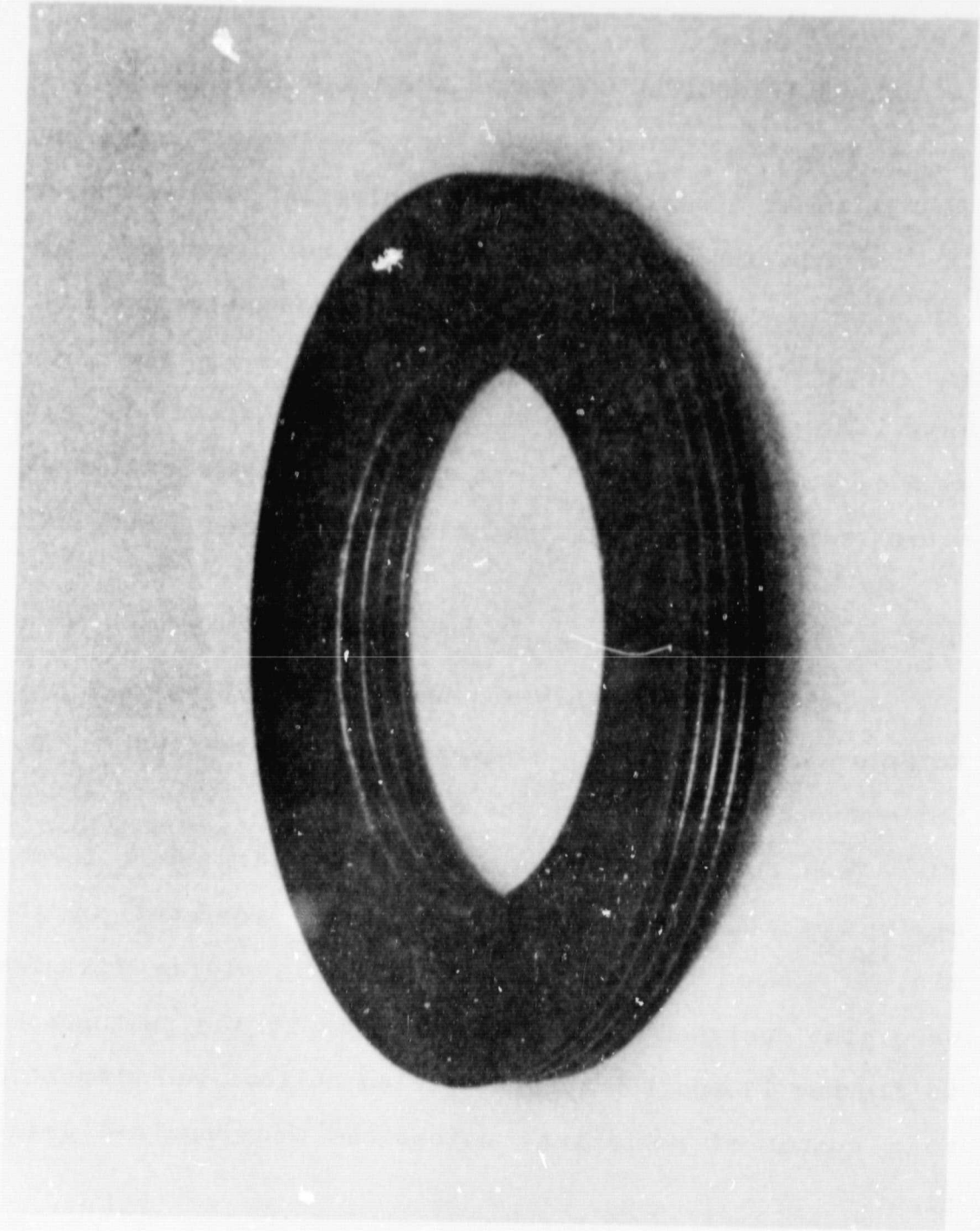


Figure 13. Photograph of Niobium Bellows

ORIGINAL PAGE IS
OF POOR QUALITY

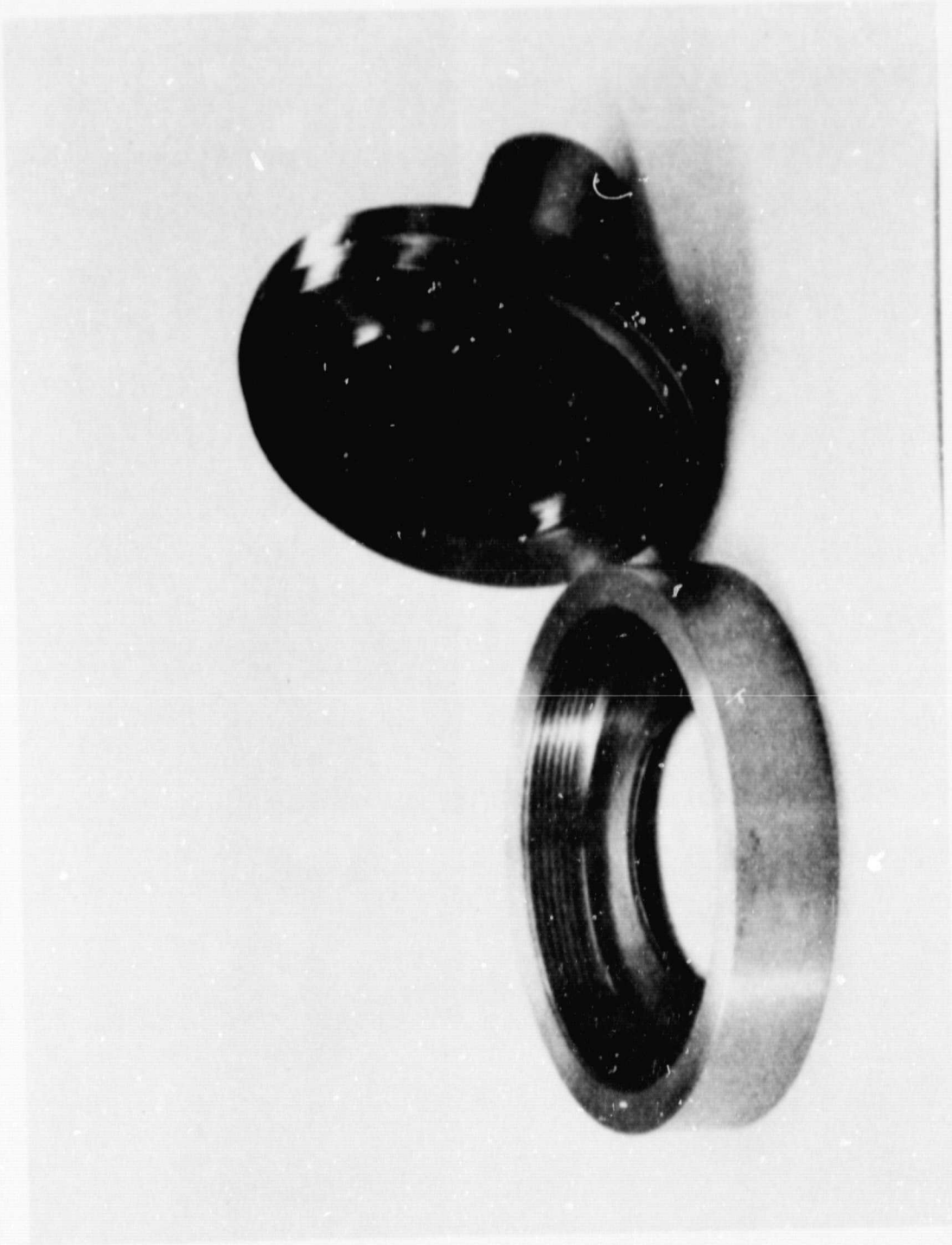


Figure 14. Electron Beam Welding Fixture

ORIGINAL PAGE IS
OF POOR QUALITY

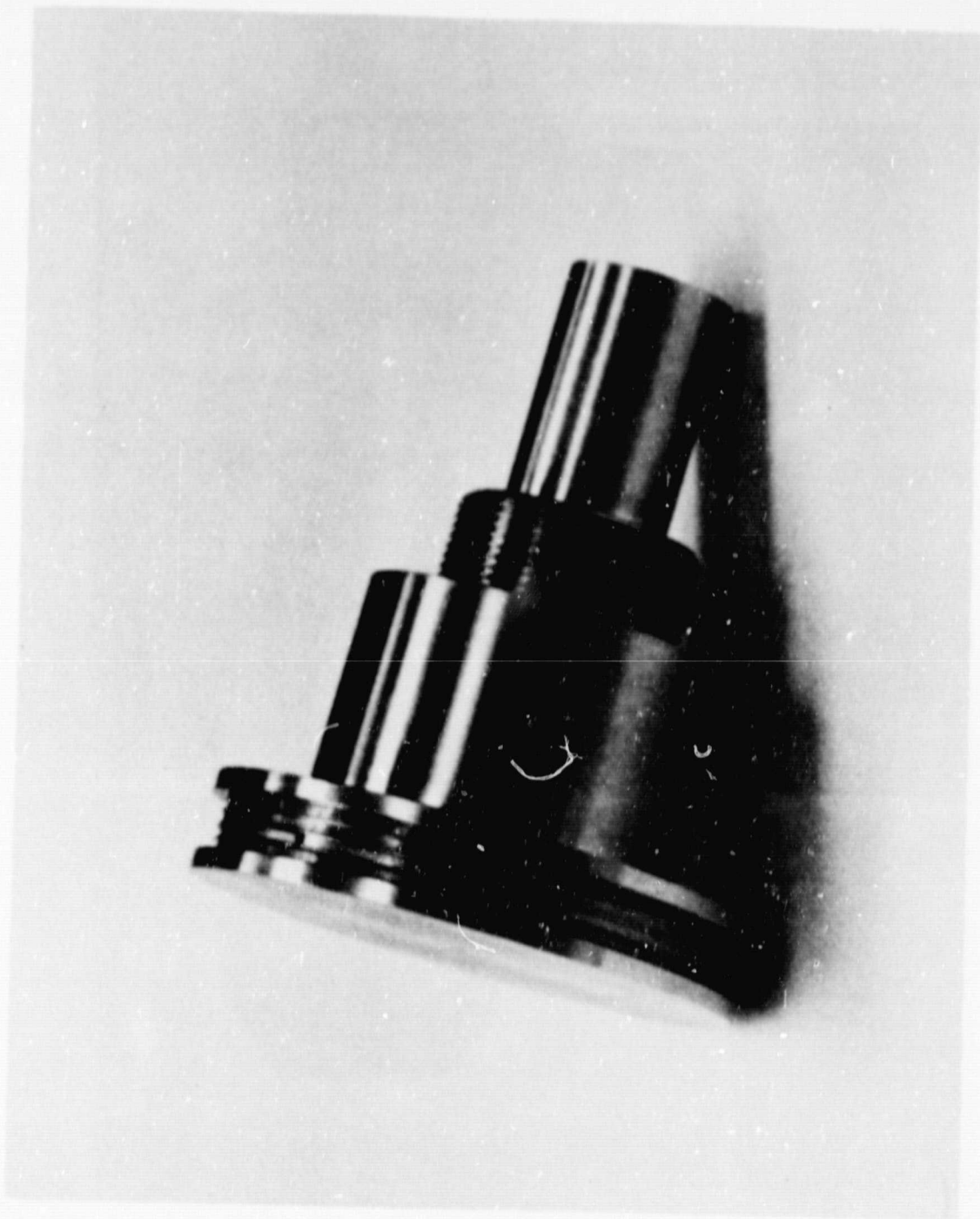


Figure 15. Assembled Electron Beam Welding Fixture

B. Emitter-Heat Pipe Electrical Insulation

The out-of-core thermionic reactor design for nuclear electric propulsion requires electrical insulation between the heat pipe and the thermionic converter at the emitter temperature (1650 K) with only a small temperature drop across the insulation. Sapphire is a candidate material for this application. Other approaches to this problem are to use a thin metal closure to the converter or to couple the heat to the converter by radiation (see Section V).

1. Evaluation of Cast Sapphire

A technique for casting sapphire between molybdenum cylinders with diameters prototypic of the NEP thermionic reactor system design was developed last year. The assembly for casting is shown in Figure 16. The sapphire reservoir is charged with crushed Lucalox, and the assembly is heated by RF in hydrogen atmosphere. The molten sapphire fills the annular gap (0.25 mm thick) between the molybdenum cylinders with the aid of the associated capillary force. Completion of the casting is signaled by the appearance of molten material at the bleed hole. After the assembly is cooled, the top and bottom were machined off and the center hole was made by electric discharge machining.

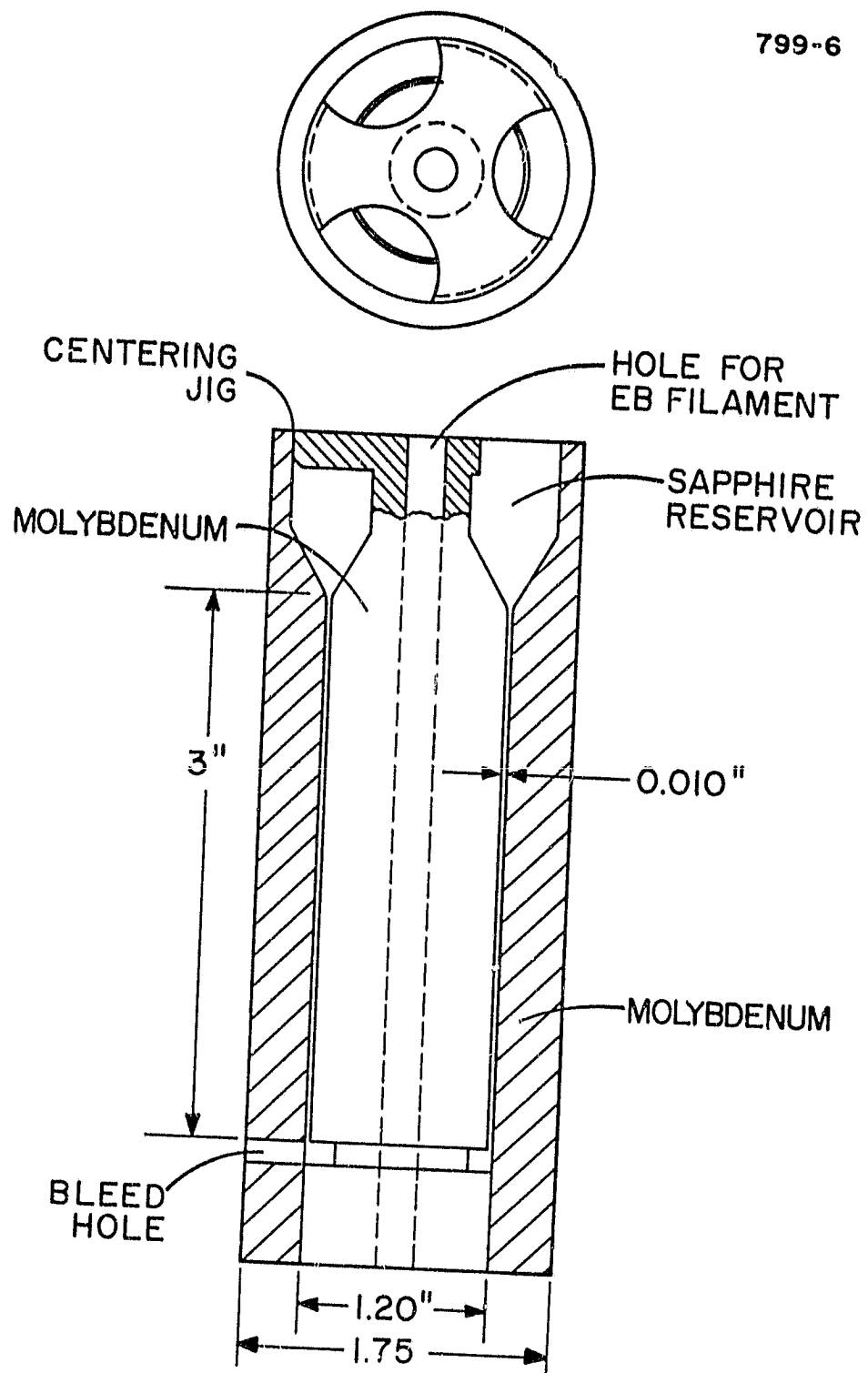


Figure 16. Assembly for Casting Sapphire

The three-inch long cylinder is mounted in a bell jar and heated by electron bombardment. A photograph of a cast sapphire unit under test is shown in Figure 17. The outside temperature was 1650 K and the temperature difference across the cast sapphire layer was approximately 20 K (measured by an optical pyrometer) at a heat flux of about 40 W/cm^2 . The outside of the unit was machined with a fine thread to increase its thermal emissivity.

The initial room temperature resistance of the first cast sapphire unit was over 10^8 ohms. The initial resistance at operating temperature (i.e., 1650 K) was two ohms. After 100 hours of testing, the room temperature resistance had decreased to about 0.1 ohms and the operating temperature resistance was almost a dead short.

After termination of the test, the unit was sectioned along the axis. Some cracks were evident, but were not in a direction to decrease heat or electrical flow. Apparently, the failure was caused by carburization of the organic fluid that penetrated the radial cracks in the cast sapphire during the electrical discharge machining. There was also evidence of sapphire-molybdenum interaction that presumably took place during the casting operation.

7910-34

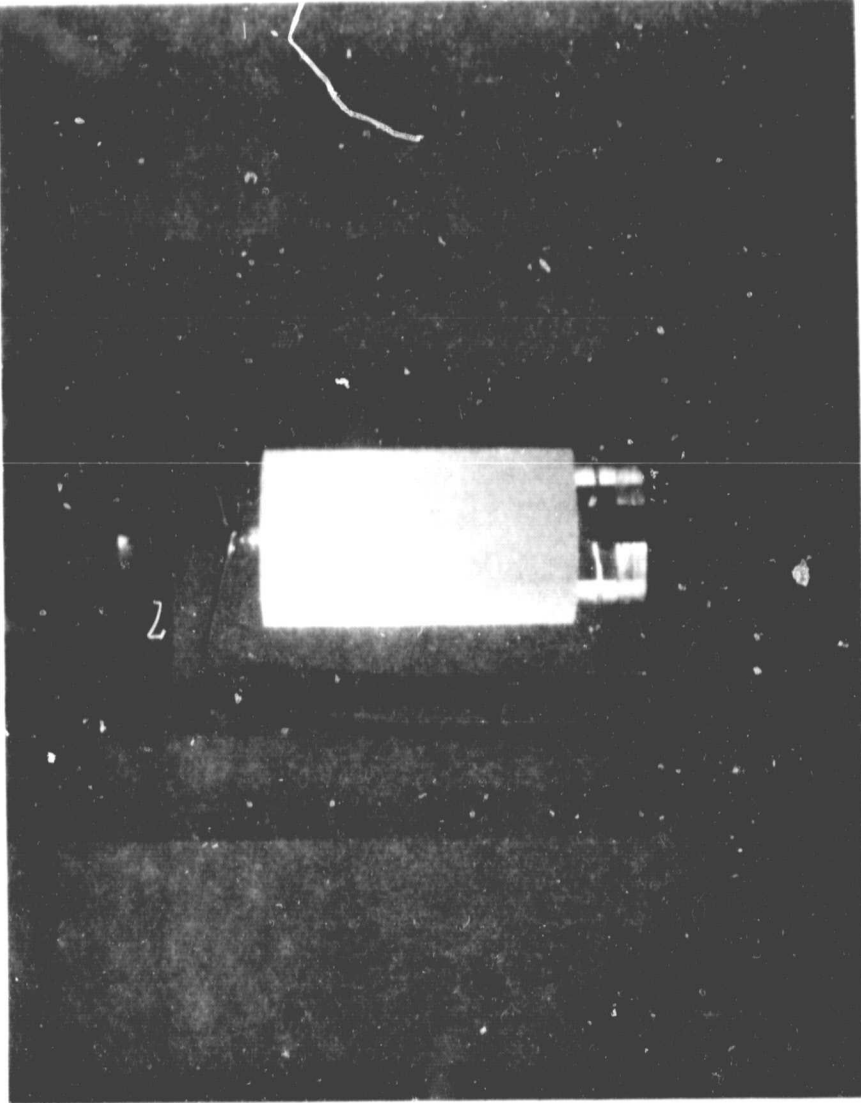


Figure 17. Cast Sapphire Assembly Under Test

The technique of casting sapphire was refined during the subject reporting period. To minimize the reaction between the alumina and molybdenum, the second casting was performed only slightly above the melting point of the alumina. Unfortunately, the alumina flow only filled the top half of the fixture.

The second unit had an initial cold resistance of 10^8 ohms and an initial hot resistance (1650 K) of approximately 120 ohms. After 30 hours of operation, the resistance stabilized at about 20 ohms. This casting was tested at 1650 K for a total of 1585 hours. During this period, a 10 volt bias was applied for 1450 hours and a 25 volt bias for 100 hours. In addition, the unit survived a 150 volt breakdown test.

On sectioning, there was no evidence of the conductive block substance found in the first casting. There was no gross interaction between the sapphire and molybdenum. Also there were fewer voids than in the first casting.

For the third test, the casting fixture was modified by drilling a hole in the bottom of the outer cylinder to provide better observation of the liquid sapphire. In addition, both molybdenum surfaces were roughened with 80

threads per inch. During the casting, the bottom of the fixture was held at a slightly higher temperature than in previous efforts to improve the flow of the sapphire. This flow was terminated as soon as it reached the bottom vent hole. Inspection showed that the sapphire flow filled the entire fixture.

The initial cold resistance was greater than 10^8 ohms and the initial resistance at 1650 K was greater than 20 ohms. However, a vacuum pump failure resulted in severe oxidation of the molybdenum and shorted the test fixture. After cleaning the apparatus and repairing the vacuum system, the unit was returned to test. However, the sapphire casting shorted at operating temperature. Efforts to clear the shorts with capacitor discharges were not successful.

Based on the foregoing experience, it appears unlikely that the cast sapphire would prove to be an adequate electrical insulator at 1650 K for the operational lives required for NEP missions.

2. Possibility of Silicon Carbide Insulation

Since silicon carbide has a band gap of approximately 3 eV, pure material would be expected to be a good electrical insulator at high temperatures. For a ceramic material, silicon carbide has a high thermal conductivity. It has a good thermal expansion match to tungsten and carbon and a fair thermal expansion match to molybdenum. In their ceramic heat pipe program, LASL has demonstrated thermal cycling to 1775 K of CVD silicon carbide on a molybdenum substrate using a thin intermediate layer of tungsten to minimize stresses. In the DOE TEC program, Thermo Electron has developed techniques of chemically vapor depositing silicon carbide on both tungsten and molybdenum using an intermediate carbon layer. These structures have operated as hot shell-emitters of combustion-fired thermionic converters for periods of 5100 hours at 1630 K and 5900 hours at 1730 K.

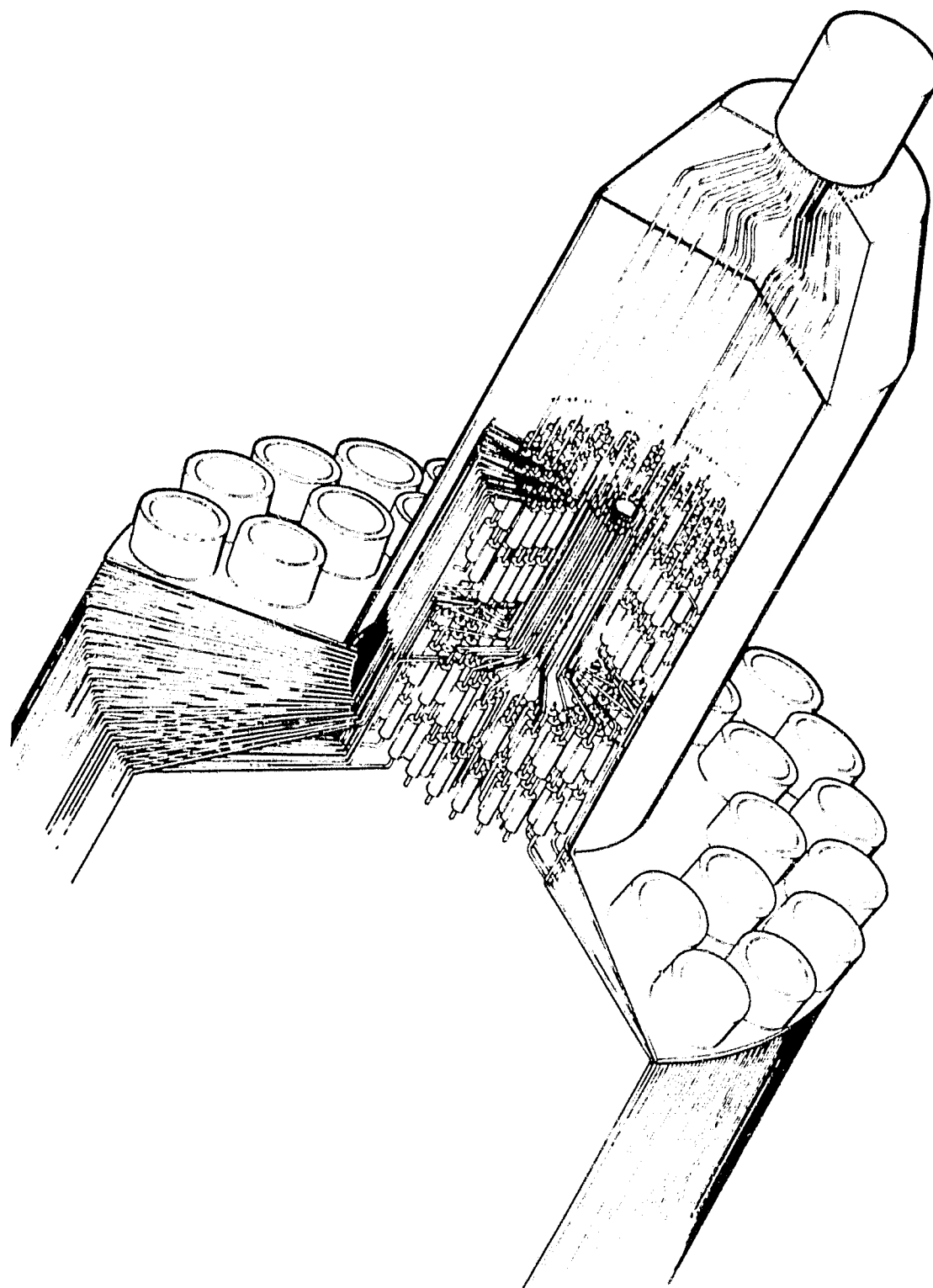
Based on these considerations, silicon carbide should be of interest as a high temperature electrical insulator. A measurement of the electrical resistivity of Thermo Electron's CVD silicon carbide at room temperature was

approximately 80 ohm-cm. This value implies a high temperature resistivity that would be too low for effective electrical insulation. However, the possibility of greatly increasing the electrical resistivity by improved purity or an additive appears promising.

V. SYSTEM CONSIDERATIONS

The system studies were directed at integrating the thermionic converter subsystem with the other power subsystems; namely the nuclear reactor, the radiator heat rejection subsystems and the power conditioning subsystem. The power system is illustrated in Figure 18. The heat from the reactor is transferred to the thermionic converters by bent lithium heat pipes, the reject heat from the thermionic converters is radiated to space by heat pipes located on the periphery of the spacecraft.

The performance goals of the system are shown in Table III. Four system configuration options were investigated as shown in Table IV. Option 1 corresponds to the illustration of Figure 18. A layout of this system option is shown in Figure 19. This figure shows the reactor, a typical lithium-molybdenum heat pipe passing through the nuclear shield and propellant storage to a typical converter. The reject heat from the converter is removed by a heat pipe. The condenser of this heat pipe forms the outer wall of the spacecraft, where the heat is radiated to space. The thermionic converters in this concept



MARCH 28, 1979

Figure 18. NEP Power Systems

SST-7

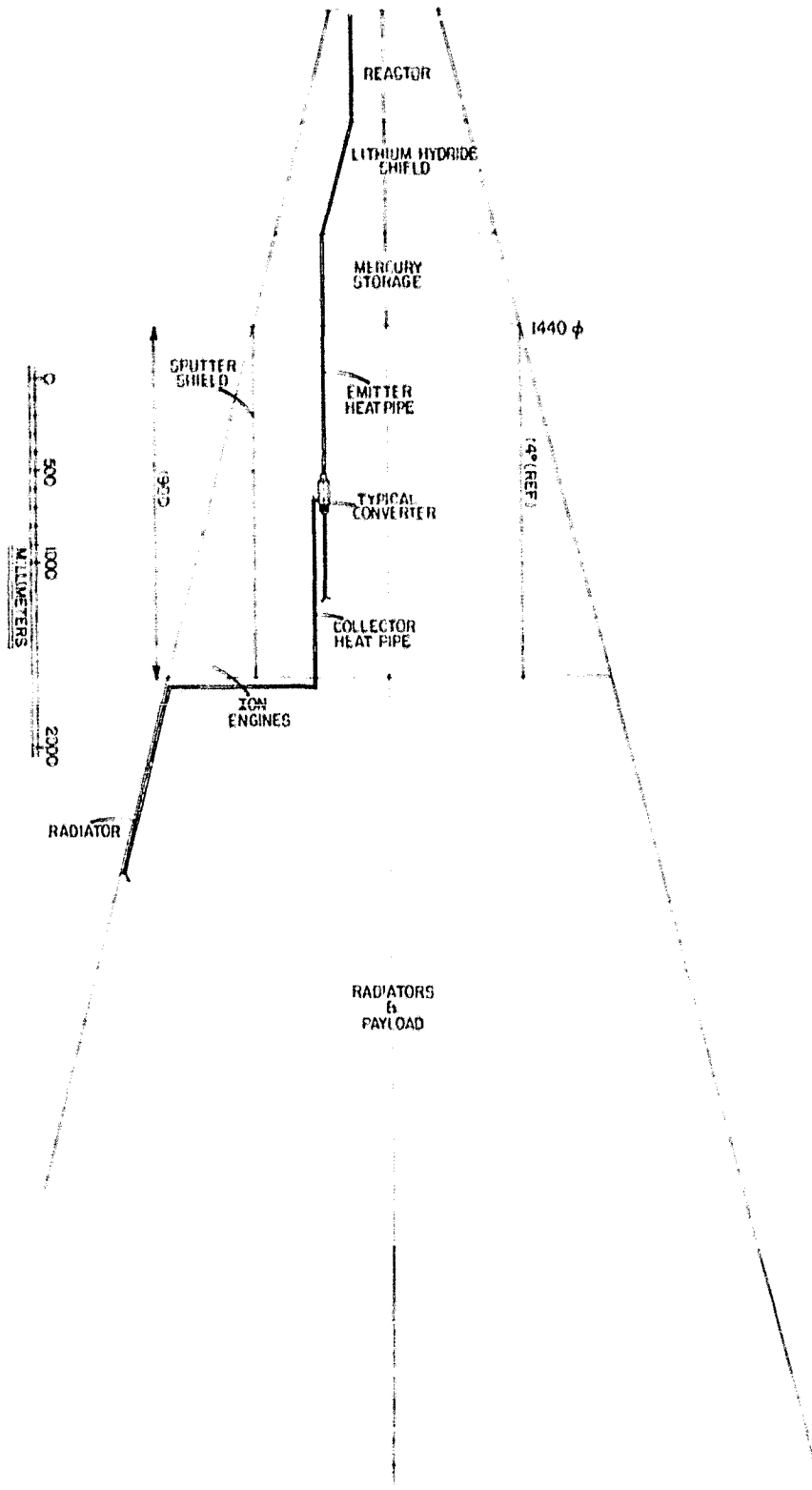
TABLE III

TEC NEP SYSTEM PERFORMANCE GOALS

- SPECIFIC MASS 22 kg/kW
- CONVERTER EFFICIENCY 12% MEASURED
- LOW MASS RADIATOR
- LONG LIFE - 40,000 HOURS MISSION LIFE
- NET POWER PRODUCED 100 TO 120 kW

TABLE IV
SYSTEM CONFIGURATIONS OPTIONS

1. INSULATED SYSTEM WITH EMITTER AND COLLECTOR HEAT PIPES
2. RADIATION COUPLED SYSTEM WITH EMITTER AND COLLECTOR HEAT PIPES
3. RADIATION COUPLED SYSTEM WITH INTEGRATED HEAT RECEIVER AND RADIATOR
4. RADIATION COUPLED SYSTEM WITH INTEGRAL HEAT RECEIVER AND RADIATOR WITH REFRACTOR WALL.



ORIGINAL PAPER IS
OF POOR QUALITY

Figure 19. Conceptual Layout of Insulated System with Emitter and Collector Heat Pipes

are electrically insulated from the reactor heat pipes, thus allowing a series-parallel connection of the converters. This results in the redundancy desired for reliability an output voltage of 32 V dc.

The projected performance of the insulated heat pipe system is shown in Figure 20, for various collector and emitter temperatures as well as differing combinations of are drop for a collector work function of 1.5 eV. The minimum power system specific mass with present day performance (i.e., $V_D = 0.5$ eV and 1700 K emitter temperature) is 20 kg/kW.

The second option considered, a radiation coupled system with emitter and collector heat pipes is geometrically similar to that shown in Figure 19. The emitter-to-heat pipe insulation, however, is replaced by a vacuum gap so that the heat transfer occurs by thermal radiation only. The available heat transport was too low to obtain a specific mass in the vicinity of 22 kg/kW.

A geometry better suited for radiation heat transfer (designed as Option 3) was investigated where the heat receiver and radiator are incorporated into the converter structure, as illustrated in Figure 21. The reactor heat

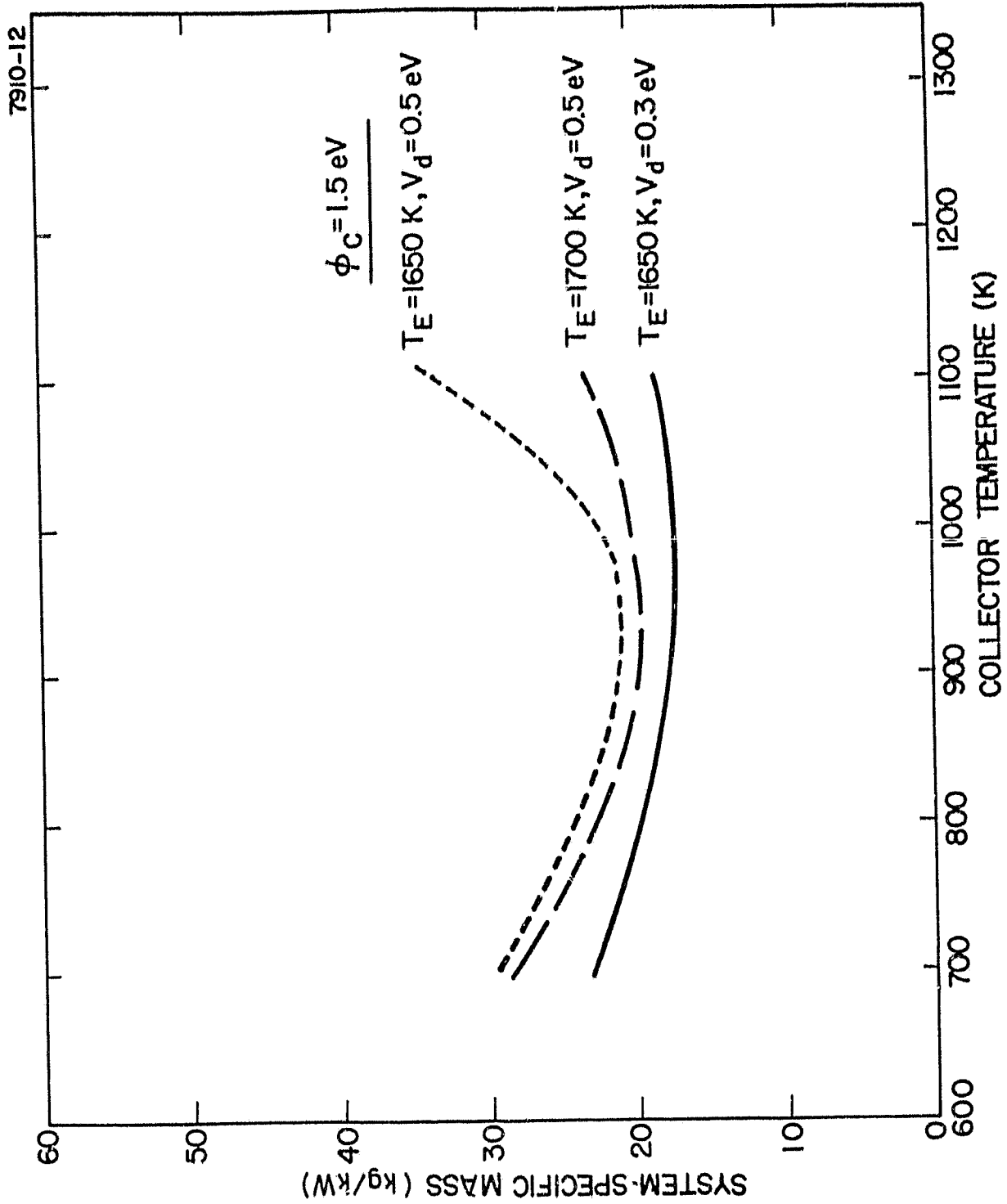


Figure 20. Specific Mass of Insulated Heat Pipe System